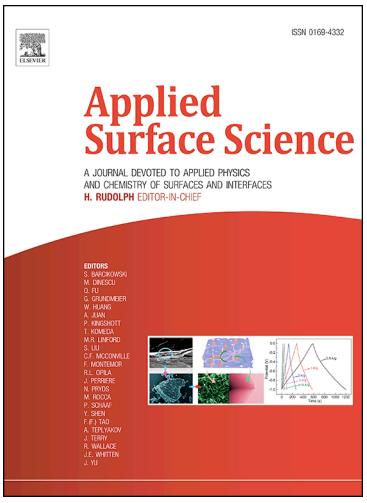

Full Length Article

Corrosion behavior of a β CuAlBe shape memory alloy containing stress induced martensite

S. Montecinos, P. Klímek, M. Sláma, S. Suarez, S. Simison

PII: S0169-4332(18)32741-7
DOI: https://doi.org/10.1016/j.apsusc.2018.10.047
Reference: APSUSC 40615

To appear in: *Applied Surface Science*

Received Date: 16 May 2018
Revised Date: 1 October 2018
Accepted Date: 4 October 2018

Please cite this article as: S. Montecinos, P. Klímek, M. Sláma, S. Suarez, S. Simison, Corrosion behavior of a β CuAlBe shape memory alloy containing stress induced martensite, *Applied Surface Science* (2018), doi: https://doi.org/10.1016/j.apsusc.2018.10.047

Corrosion behavior of a β CuAlBe shape memory alloy containing stress induced martensite

S. Montecinos[a, b], P. Klímek[c], M. Sláma[c, d], S. Suarez[e], S. Simison[b, f]

[a] Instituto de Física de Materiales Tandil-IFIMAT, Facultad de Ciencias Exactas, Universidad Nacional del Centro de la Provincia de Buenos Aires, Pinto 399, 7000 Tandil, Argentina.

[b] CONICET, Godoy Cruz 2290 CABA, Argentina.

[C] TescanOrsay Holding a.s., Libusina trida. 863/21, 623 00 Brno, Czech Republic.

[d] Institute of Materials Science and Engineering, Brno University of Technology, Technicka 2, 616 00 Brno, Czech Republic.

[e] Functional Materials, Dept. Materials Science & Engineering, Saarland University. Campus D3 3, D-66123 Saarbrücken, Germany.

[f] INTEMA, Facultad de Ingeniería, Universidad Nacional de Mar del Plata, Juan B. Justo 4302, 7600 Mar del Plata, Argentina.

Abstract

The corrosion behavior of a β CuAlBe shape memory alloy containing stress-induced martensite was analyzed after 60 days of immersion in a 3.5 % NaCl solution. The stress-induced martensite was retained in the sample after a load-unload compression cycle up to a pseudoelastic deformation of 4.5 %. The corrosion of the alloy occurs by dealuminization, where β phase located in the areas between the needles of martensite is dissolved due to the preferential loss of aluminum, and the posterior redeposition of copper takes place.

Keywords: Dealloying; retained martensite; Cu-based alloys; microstructure; shape memory alloys.

1. Introduction

The Cu-11.4Al (wt.%) system with small additions of beryllium exhibits shape memory properties due to the martensitic transformation (MT). At high temperatures, β phase is stable with a disordered structure, however, it can be retained at low temperatures by rapid cooling [1-2]. The disordered β phase orders to a DO_3 structure during cooling [3]. Under slow cooling from high temperature, the metastable β phase decomposes into the phases γ_2 and α', with high and low aluminum content respectively [1, 4].

The martensitic transformation from β phase to 18R martensite can be induced by cooling, spontaneous transformation, or under mechanical stress. The spontaneous transformation occurs with the formation of 24 self-accommodates variants of 18R martensite without macroscopic change of shape. It begins at a martensite-start temperature (Ms). The martensite variants have identical crystal lattice but they can appear in different orientations. By the application of mechanical stress, on tension or compression, β phase transforms to 18R martensite with a macroscopical change of shape [5]. When the material in β phase is subjected to stress, it first elastically deforms and for higher stresses the martensitic transformation of β to 18R martensite is carried out. The stress corresponding to the end of the linear elastic regime is usually referred as the martensite-start stress (σ_s). The sample in β phase is loaded up to a maximum stress (σ_{max}) and then the load is removed. Under appropriate conditions, a hysteretic loop is obtained after unloading with almost complete strain recovery, leading to a pseudoelastic cycle. The pseudoelastic strain (ε_{ps}) can be define as the total applied strain discounting the elastic contribution [5]. There is a limit for the complete recovery of the applied deformation, which depends among other factors on the microstructural characteristics of the sample, the experimental conditions and the composition of the alloy. From therein more, strain is increasingly retained on unloading, due to the presence of martensite needles that could not retransform to β phase and remain retained

in the sample. When the material does not fully recover the deformation, a retained strain (ε_{ret}) is observed on unloading. The CuAlBe alloy can exhibit the pseudoelastic behavior at room temperature [5-9]. The hysteretic loop is associated to the dissipation of mechanical energy into heat. Because of these characteristics, the use of CuAlBe alloys as passive dampers of seismic energy is highly promising [6-7, 10-12].

Copper alloys present low corrosion susceptibility, so, they are widely used in marine environments. The aluminum addition improves their corrosion resistance in chloride media, because it makes the corrosion product film to become more protective [13-16]. Previous studies in CuAlBe alloy in chloride containing environments have shown that the corrosion process occurs by dealuminization, where aluminum is preferentially removed from the alloy [17-19]. This process has been also reported in CuAl and CuAlX alloys in chloride media [13]. The corrosion behavior of CuAlBe alloys has been studied when they were immersed in a 3.5 % NaCl for different times up to 40 days, and by electrochemical tests [17-19]. The influence of the microstructure, specifically the presence of precipitates with different composition to the β matrix was investigated in detail. In samples with γ_2 phase, the preferential dissolution of the precipitates occurs, protecting the matrix from dealloying [17]. On the other hand, the copper-rich precipitates, α', exhibit a high corrosion stability [19].

In the present study the corrosion behavior of a β CuAlBe shape memory alloy containing stress induced martensite in a 3.5 % NaCl solution adjusted to pH 8 was analyzed, in view of its application as seismic dampers in bridges. This condition is intended to be a simple approximation for a sea water environment.

2. Experimental procedure

A commercial Cu-11.40Al-0.55Be (wt.%) polycrystalline alloy, provided by Trefimetaux S.A. as 15 mm diameter extruded bars, was used in the present work. The chemical composition was determined by atomic absorption spectrophotometry. Samples of square section of around 5×5 mm^2 and 15.9 mm length were cut using an Isomet Low Speed Saw with a diamond disc. To make sure that the samples are in β phase at room temperature, they were kept during 10 min in a resistance furnace at 1073 K, and water quenched at room temperature. A mean grain size of 0.8 mm was obtained, and a temperature Ms around 259 K was determined by calorimetric measurements.

Compression tests were carried out at room temperature with a Shimadzu Autograph-DSS-10T universal testing machine with deformation control and using a load cell of 10 ton. A constant cross-head speed of 1 mm/min was used. To reduce the friction between the specimen faces and the compression module, the end faces were covered with a thin Teflon film and lubricated with grease. After the mechanical tests, samples were characterized by optical microscopy, using a Reichert MeF2 microscope. In order to reveal the microstructural details, the specimens were electropolished at 4 V in a saturated solution of chromium trioxide in phosphoric acid, and immersed for 5 seconds in a solution of ferric chloride.

Before the immersion, samples were smoothed with 1000 grit emery paper. Specimens were immersed for 60 days in a 3.5 % NaCl solution adjusted to pH 8 with borate-boric acid buffer. The solution was maintained at room temperature, and air was bubbled through it. After the immersion, the surface of the samples was rinsed softly with distilled water, sprayed with ethanol and dried with warm air. The surface morphology of the specimens was examined using an Olympus BX60 microscope (OM), and a JEOL JSM-6460LV scanning electron microscope (SEM). To estimate the surface composition of different zones of the samples, energy dispersive X-ray spectroscopy

(EDX) analysis under SEM was employed. To identify the phase structure of the corrosion products film formed during the immersion, X-ray diffraction (XRD) measurements were carried out using a PANanalytical X'Pert Pro PW3373 and a PANanalytical X'Pert MPD X-ray diffractometers with normal and low incident angle.

TOF-SIMS and EBSD Analysis

In the TOF-SIMS analysis C-TOF (TofWerk, Thun, Switzerland) integrated on FIB-SEM Tescan LYRA3 (Tescan Orsay Holding., Brno, Czech Republic) was used. For investigation of crystallographic nature, EBSD camera NordlysMax^3 (Oxford instruments, Abingdon, United Kingdom) was employed. Prior to both analyses, a cube with dimensions 20×20×20 μm^3 from a specific position on sample was prepared (Figure 1(a)). Subsequently, the prepared cube was lifted out from the base material to get optimal conditions of signal for both types of analysis without shielding effects. For preparation of the cube, trenches were milled around with stairs trench milling strategy (as defined in TESCAN Drawbeam tool) with a 25 nA ion beam current at accelerating voltage 30 kV (Figure 1(a)). A SmarAct nano-manipulator was used for lift out the cube and it was attached to a TEM grid (Figure 1(b)). Then, the area of interest was polished using an ion beam current of 100 pA at accelerating voltage 30 kV in order to enhance the diffraction pattern contrast, necessary for subsequent EBSD analysis.

On such surface (Figure 1(c)) grain orientation and phases present were investigated and evaluated with Aztec EBSD software (Oxford instruments, Abingdon, United Kingdom). During the analysis current of the electron beam was 8 nA at accelerating voltage 30 kV (measured as absorbed current with Faraday cup in SEMs stage).

After the EBSD analysis was made, the same area was analyzed with TOF-SIMS. In TOF-SIMS analysis, the area of interest with dimensions 12×12 μm^2 was scanned. While Ga^+ primary focused ion beam was scanning over the area with the beam current of 200 pA at accelerating voltage 30 kV, secondary ions were simultaneously analyzed with C-TOF in positive mode. The results were represented as elemental distribution maps derived from 70 scans of the area of interest.

FIGURE 1

3. Results and discussion

The samples in β phase were subjected to compression tests at a maximum stress $\sigma_{max} \approx$ 300 MPa to induce martensite phase. The obtained stress-strain (σ-ε) curve is shown in Figure 2(a). The first linear part in the loading curve is the elastic region of the β phase, and the deviation of the linearity is associated with the beginning of the transformation of β to martensite. Then, the martensitic transformation continues up to σ_{max}. On removing the load, the retransformation of martensite to β phase occurs, and a hysteretic loop is formed. An almost complete strain recovery is expected up to ε_{ps} around 3 % [20]. As σ_{max} increases, the induced martensite cannot completely retransform to β phase. In our case a retained strain (ε_{ret}) of 0.8 % was obtained for ε_{ps}=4.5 %. That level of deformation was chosen considering that for an optimal use of the material as passive damping devices, it is required that it would be subjected to sufficiently high deformations to achieve the damping of the greatest amount of energy, but not so high to retain so much martensite needles after the unloading. A micrograph of the sample after the compression cycle is presented in Figure 2(b). The presence of retained stress-induced martensite as a crosslinked network of fine needles in the β matrix is observed. The martensite needles exhibit widths between about 0.5 and 10 μm. The volume

fraction of retained martensite was estimated from the strain retained data as 6 ± 2 %, using the relationship between both parameters reported in reference [5]. The fraction of martensite was also obtained from optical micrographs as 11 ± 3 %. This procedure is that commonly used for determination of volume fractions of individual phases [21].

FIGURE 2

After the immersion, the surface of the samples was examined by optical microscopy and SEM with EDX (Figure 3). Preferential dissolution of the β phase located in the areas between the needles of martensite is observed (Figure 3(a)). This fact is more evident in the micrographs obtained from a cross-section (Figure 3(b)), especially in that obtained by SEM in the inset, where a representative corrosion depth of around 10 μm is observed. The EDX analysis results of different zones are given in Table 1. According to EDX results, the martensite needles remain uncorroded. On the sample surface, some corrosion products based on O were detected, and copper particles with sizes up to around 50 μm were found (with ≈ 98 wt.% Cu). They can be observed on top of the uncorroded martensite needles (Figure 3(b)). The copper crystals would be formed by a dissolution-redeposition mechanism as has been previously reported [16-17, 22]. EBSD map of the redeposited crystals shows they correspond to copper cubic phase consisting of grains with different crystallographic orientations (Figure 4).

Table 1. EDX analysis of different zones in Figure 3.

Element	**Mass concentration (wt.%)**	
	Cu particles	**Matrix (Zone 1)**
Cu	98.18	77.03
Al	0.36	13.24
O	1.47	9.73

FIGURE 3

FIGURE 4

The diffraction patterns of the sample after immersion are presented in Figure 5. The presence of Cu particles on the surface of the sample is confirmed, and they are also detected in the pattern obtained from the cross-section. The existence of corrosion products based on Al, O and Cl on the surface of the samples is confirmed: Al_2O_3, $CuO{\cdot}Cu_2O$, CuO, and $CuCl_2$. A TOF-SIMS analysis of the cross-section of the sample after immersion was carried out. The element distribution maps of Al, Be and O are presented in Figure 6. It can be observed the presence of Al and O on the surface of the corroded sample, which is in agreement with the presence of some oxides of copper and Al_2O_3. Some quantities of Beryllium, greater than those present in the original alloy, could be also detected by TOF-SIMS analysis on the surface of the sample, which indicates the formation of some Be compounds as corrosion product. It is important to note that the presence of Be had not been detected by any other technique, due to technical difficulties on its determination. However, more work is needed in order to determine the beryllium compounds that are formed.

FIGURE 5

FIGURE 6

When a β sample is subjected to mechanical stress, the martensitic transformation is induced, and needles are formed in the most favored directions in each grain. It is important to note that during a uniaxial test on a polycrystalline specimen, stresses in many directions are induced. After the unloading, some needles of martensite can be retained. Their presence can deteriorate the pseudoelastic behavior of the material, leading to a decrease in the stress for the beginning of the martensitic transformation, and an increase in the strain retained on unloading [5]. However, there is no knowledge about the possible influence of the martensite on the corrosion behavior, especially in marine environments. In this work, we found that the martensite needles remain practically uncorroded while the β matrix suffers dealloying and higher corrosion rates.

The β matrix corresponds to a long range ordered DO_3 structure [3]. The β to 18R martensite transformation is induced by stress, and the formed martensite phase has a long-range order inherited from the β matrix. It is important to note that no compositional change takes place during the martensitic transformation, and both phases, β and martensite have the same composition but different crystalline structure. The structure of the 18R martensite is an ordered orthorhombic lattice consisting of 18 close-packed layers in each period. This structure is generated by introducing stacking faults on each third plane, with a stacking sequence AB'CB'CA'CA'BA'BC'BC'AC'AB' [1, 23-24]. The better corrosion resistance of martensite needles than the β matrix could be due to the difference in the concentration of defects in both phases. Due to the nature of the martensitic transformation, a high density of stacking faults are formed in the 18R martensite to adjust the interface with the β phase to a plane of invariant habit [25].

In a previous work it was found that the corrosion of CuAlBe alloys in 3.5 % NaCl occurs by dealuminization [17-19]. After 60 days of immersion, β phase located in the areas between the needles of martensite is dissolved due to the preferential loss of aluminum, and the posterior dissolution-redeposition of copper takes place. This process is evidenced by the presence of copper crystals on the surface of the sample, corresponding to polycrystalline particles. Based on the XRD and TOF-SIMS results, the aluminum dissolution leads to the formation of Al_2O_3, and the corrosion products Cu_2O/CuO and CuO are also present on the surface. These results are in agreement with the fact that the main anodic reaction would be the formation of oxides of copper and aluminum oxides/hydroxides and the oxygen reduction would be the main cathodic reactions. Al_2O_3 would be formed by the complexation of aluminum by chloride and a subsequent hydrolysis [26]. Previous studies of copper in chloride media have found that the first corrosion product of copper is cuprous chloride, CuCl, which produces cuprous oxide, Cu_2O, and it oxides to CuO at higher potential [17, 19, 27]. It was also found the presence of $CuCl_2$, which has been also reported by other authors, especially on cyclic voltammetric time-scales [19, 28-29].

In the XRD measurements obtained from the cross-section of the sample (Figure 5(b)), the presence of Cu, β phase and Al_2O_3 is detected. β phase corresponds to the non-corroded matrix, far from the surface of the sample. The Cu signal would correspond to the crystals on the surface of the sample, and some severely corroded grains inside the specimen. Those grains suffer dealuminization, obtaining a porous matrix rich in copper. The Al_2O_3 detected would correspond to a corrosion product located in the zones where the β phase was dissolved. The presence of some Be compounds on the surface of the samples was also detected by TOF-SIMS analysis.

Only a few studies have compared the corrosion behavior of β and martensite phases in CuAl shape memory alloys. Raheem et al. [30] studied the corrosion behavior of CuAlNi shape memory alloys immersed in a NaOH solution, and they also found a higher resistance of the alloy in martensitic phase respect to the β alloy. The alloy in martensitic phase was obtained by specific heat treatments. The alloy in martensitic phase was obtained by specific heat treatments. The present study includes the results obtained in a first insight on the influence of stress-induced martensite on the corrosion behavior in chloride environment of a β CuAlBe shape memory alloy. More work is needed in order to understand the specific role of the stacking faults on the corrosion protection of the martensite phase.

4. Conclusions

The influence of the stress-induced martensite on the corrosion behavior of a β CuAlBe shape memory alloy after 60 days of immersion in a 3.5 % NaCl solution was analyzed, in view of its application as seismic dampers in bridges due to the pseudoelastic behavior. After a pseudoelastic cycle, some of the stress-induced martensite needles could not retransform to β phase and remain retained in the sample. From there arises the importance of the study of β CuAlBe alloys containing stress-induced martensite. The martensite needles were retained in the sample after a load-unload compression cycle up to a pseudoelastic deformation of 4.5 %.

The surface morphology of the specimens after immersion was examined in detail using different surface characterization techniques. The corrosion of the alloy occurs by dealuminization, where β phase located in the areas between the needles of martensite is dissolved, and the posterior redeposition of copper takes place. This process is evidenced by the presence of copper crystals on the surface of the sample, corresponding to polycrystalline particles. The aluminum forms Al_2O_3, and the corrosion products Cu_2O/CuO and CuO are also present on the surface. The existence of some Be compounds on the surface of the samples was also detected by TOF-SIMS analysis.

This study includes the first results obtained on this subject, where the martensite needles remain practically uncorroded while the β matrix suffers dealloying and higher corrosion rates. The better corrosion resistance of martensite needles than the matrix could be due to the difference in the concentration of defects in both phases. More work is needed in order to understand the origin of the corrosion resistance of the martensite phase.

Acknowledgements

This work was supported by ANPCYT, CONICET, Universidad Nacional de Mar del Plata, and SECAT-UNCPBA. The authors would also like to thank to Dr. Mariela Desimone for her collaboration with the XRD measurements.

References

[1] S. Belkahla, H. Flores Zuñiga, G. Guenin, Elaboration and characterization of new low temperature shape memory Cu-Al-Be alloys, Mater. Sci. Eng. A 169 (1993) 119-124.

[2] P.R. Swan, H. Warlimont, The electron metallography and crystallography of copper-aluminum martensites, Acta Met. 11 (1963) 511-527.

[3] M. Jurado, T. Castán, L.L. Mañosa, A. Planes, J. Bassas, X. Alcobé, M. Morin, Study of the order-disorder phase transitions in Cu– Al–Be shape memory alloys, Philos. Mag. A 75 (1997) 1237-1250.

[4] S. Montecinos, A. Cuniberti, M.L. Castro, R. Boeri, Phase transformations during continuous cooling of polycrystalline β-CuAlBe alloys, J. Alloys Compd. 467 (2009) 278-283.
[5] S. Montecinos, A. Cuniberti, A. Sepúlveda, Grain size and pseudoelastic behaviour of a Cu-Al-Be alloy, Mater. Charact. 59 (2008) 117-123.
[6] S. Montecinos, A. Cuniberti, Thermomechanical behavior of a CuAlBe shape memory alloy, J. Alloys Compd. 457 (2008) 332-336.
[7] S. Montecinos, Influence of microstructural parameters on damping capacity in CuAlBe shape memory alloys, Mater. Des. 68 (2015) 215-220.
[8] B. Kaouache, S. Berveiller, K. Inal, A. Eberhardt, E. Patoor, Stress analysis of martensitic transformation in Cu-Al-Be polycrystalline and single-crystalline shape memory alloy, Mater. Sci. Eng. A 378 (2004) 232-237.
[9] A. Hautcoeur, A. Eberhardt, E. Patoor, M. Berveiller, Thermomechanical behaviour of monocrystalline Cu-Al-Be shape memory alloys and determination of the metastable phase diagram, J. Phys. IV C2 5 (1995) 459-464.
[10] A. Isalgue, J. Fernandez, V. Torra, F.C. Lovey, Conditioning treatments of Cu-Al-Be shape memory alloys for dampers, Mater. Sci. Eng. A 438-440 (2006) 1085-1088.
[11] R. Desroches, B. Smith, Shape memory alloys in seismic resistant design and retrofit: a critical review of their potential and limitations, J. Earthquake Eng. 7(3) (2003) 1-15.
[12] J.M. Jani, M. Leary, A. Subic, M.A. Gibson, A review of shape memory alloy research, applications and opportunities, Mater. Des. 56 (2014) 1078-1113.
[13] A.V. Benedetti, R.T.A. Sumodjo, K. Nobe, P.L. Cabot, W.G. Proud, Electrochemical studies of copper, copper-aluminium and copper-aluminium-silver alloys: Impedance results in 0.5 M NaCl, Electrochim. Acta 40 (16) (1995) 257-2668.
[14] H. Wojtas, S. Virtanen, H. Böhni, Electrochemical characterization of new stainless Cu-Al-Sn alloys, Corr. Sci. 37(5) (1995) 793-799.
[15] Z. Han, Y.F. He, H.C. Lin, Dealloying characterizations of Cu-Al alloy in marine environment, J. Mater. Sci. Lett. 19 (2000) 393-395.
[16] J.A. Wharton, K.R. Stokes, The influence of nickel-aluminium bronze microstructure and crevice solution on the initiation of crevice corrosion, Electrochim. Acta 53 (2008) 2463-2473.
[17] S. Montecinos, S. Simison, Influence of the microstructure on the corrosion behavior of a shape memory Cu-Al-Be alloy in a marine environment, Appl. Surf. Sci. 257 (2011) 2737-2744.
[18] S. Montecinos, S. Simison, Corrosion behavior of Cu-Al-Be shape memory alloys with different compositions and microstructures, Corros. Sci. 74 (2013) 387-395.
[19] S. Montecinos, S.N. Simison, Study of the corrosion products formed on a multiphase CuAlBe alloy in a sodium chloride solution by micro-Raman and in situ AFM measurements, Appl. Surf. Sci. 257 (2011) 7732-7738.
[20] S. Montecinos, A. Cuniberti, Effects of grain size on plastic deformation in a β CuAlBe shape memory alloy, Mater. Sci. Eng. A 600 (2014) 176-180.
[21] G.F. Vander Voort, Metallography: Principles and Practice, McGraw-Hill Book Co., New York, 1984.
[22] R. Davis, Metals Handbook: Volume 13-Corrosion, ninth edition, ASM International, Metals Park, Ohio, 1987.
[23] S. Kajiwara, An X-Ray study of faulting in martensite of Cu-Al alloys, Jpn. J. Appl. Phys. 7(4) (1968) 342-347.
[24] H. Warlimont, M. Wilkens, Die struktur der martensitphase β-1 im system kupfer-aluminium, Z. Metallkunde 55 (1964) 382-387.

[25] K. Otsuka, C.M. Wayman, Shape memory materials, Cambridge University Press, Cambridge, United Kingdom, 1998.
[26] M. Wang, Y. Zhang, M. Muhammed, Critical evaluation of thermodynamics of complex formation of metal ions in aqueous solutions. III. The system Cu(I.II)-Cl^-e at 298.15 K, Hydrometallurgy 45 (1997) 53-72.
[27] G. Kear, B.D. Barker, F.C. Walsh, Electrochemical corrosion of unalloyed copper in chloride media-a critical review, Corros. Sci. 46 (2004) 109-135.
[28] R. Procaccini, W.H. Schreiner, M. Vázquez, S. Ceré, Surface study of films formed on copper and brass at open circuit potential, Appl. Surf. Sci. 268 (2013) 171-178.
[29] A.G. Christy, A. Lowe, V. Otieno-Alego, M. Stoll, R.D. Webster, Voltammetric and Raman microespectroscopic studies on artificial copper pits grown in simulated potable water, J. Appl. Electrochem. 34 (2004) 225-233.
[30] A. Raheem, K.A. Ali, Z.T. Al-Tai, The effect of iron addition on the dry sliding wear and corrosion behavior of CuAlNi shape memory alloy, Eng. Tech. J. 28(24) (2010) 6888-6902.

Figure Captions

Figure 1. Cube prepared for lift out (a), cube before polishing attached to a TEM grid (b), polished surface of an area of interest (c).

Figure 2. (a) Stress-strain curve for the sample in β phase subjected to a single cycle of compression. (b) Optical micrograph of the sample after the compression cycle.

Figure 3. Micrographs of a CuAlBe sample subjected to a compression cycle and immersed in a NaCl solution for 60 days. (a) SEM image, (b) micrograph obtained by OM from the cross section of the sample. The inset in Figure (b) corresponds to an image obtained by SEM.

Figure 4. (a) EBSD band map from the cross section of the sample showing the redeposited copper crystals, and (b) EBSD crystal map showing the different crystallographic orientation.

Figure 5. XRD patterns of the sample after 60 days of immersion in 3.5 % NaCl. (b) was obtained from the cross-section.

Figure 6. Element distribution maps obtained by TOF-SIMS analysis of the cross-section of the sample after 60 days of immersion in 3.5 % NaCl. The micrograph at the bottom corresponds to the SEM image captured before TOF-SIMS analysis.

Research highlights

The corrosion behavior of a β CuAlBe with stress-induced martensite was analyzed

The corrosion of the alloy occurs by dealuminization and redeposition of Cu

β phase located in the areas between the needles of martensite is dissolved

Corrosion products are present in the surface: Cu crystals, Cu-oxides and Al_2O_3